Creep analysis of an earth embankment on soft soil deposit with and without PVD improvement

Rezania, M., Bagheri, M., Mousavi Nezhad, M. & Sivasithamparam, N.

Original citation & hyperlink:
Rezania, M, Bagheri, M, Mousavi Nezhad, M & Sivasithamparam, N 2017, 'Creep analysis of an earth embankment on soft soil deposit with and without PVD improvement' Geotextiles & Geomembranes, vol. 45, no. 5, pp. 537-547. https://dx.doi.org/10.1016/j.geotexmem.2017.07.004

DOI 10.1016/j.geotexmem.2017.07.004
ISSN 0266-1144

Publisher: Elsevier

Creep analysis of an earth embankment on a soft soil deposit with and without PVD improvement

Mohammad Rezania[a,*,1], Meghdad Bagheri[b,2], Mohaddeseh Mousavi Nezhad[a,3], Nallathamby Sivasithamparam[c,4]

[a]School of Engineering, University of Warwick, Coventry, UK

[b]Department of Civil Engineering, University of Nottingham, Nottingham, UK

[c]Computational Geomechanics Division, Norwegian Geotechnical Institute, Oslo, Norway

Abstract

In this paper, an anisotropic creep constitutive model, namely Creep-SCLAY1S is employed to study the installation effects of prefabricated vertical drains (PVDs) on the behavior of a full scale test embankment, namely Haarajoki embankment in Finland. Half of the embankment is constructed on unimproved natural soft soil while its other half is constructed on the PVD improved soil foundation. The Creep constitutive model, used in this study, incorporates the effects of fabric anisotropy, structure and time within a critical state based framework. For comparison, the isotropic modified Cam clay (MCC) model and the rate-independent anisotropic S-CLAY1S model are also used for the analyses. The results of the numerical analyses are compared with the field measurements. Based on the results it is found that the creep model provides an improved approximation of settlements and excess pore pressure dissipations. In addition, the application of two commonly used permeability matching techniques for two dimensional (2D) plane-strain analysis of the PVD problem is studied and the results are discussed in detail.

*,[1]Corresponding author. E-mail address: m.rezania@warwick.ac.uk. Tel.: +44 24 76 522339.

[2] E-mail address: meghdad.bagheri@nottingham.ac.uk. Tel.: +44 115 95 12850.

[3] E-mail address: m.mousavi-nezhad@warwick.ac.uk. Tel.: +44 24 765 22332.

[4] E-mail address: nallathamby.siva@ngi.no. Tel.: +47 406 94 933.

Keywords: Geosynthetics; Embankment; PVDs; Soft clay; Creep behavior; Advanced constitutive modeling

1 Introduction

In order to tackle the delayed consolidation settlement problem typical of soft soils, installation of prefabricated vertical drains (PVDs), combined with preloading, has become popular in the industry as an effective ground improvement solution (e.g. Abuel-Naga et al. 2015, Lam et al. 2015, Wang et al. 2016). Preloading is an old way of dealing with the problem of long-term consolidation in soft soils; however, in practice, this procedure on its own can be considerably time consuming. For the excess pore water pressure (PWP) to be dissipated quickly, the drainage paths need to be shortened. PVDs are geosynthetic slender elements made of corrugated plastic cores that their Installation can effectively reduce the consolidation time as they provide short horizontal drainage paths in thick soft soil deposits that need improvement (Rowe and Taechakumthorn 2008).

Some aspects of PVD installation e.g., well resistance, smear effect and the overlapping of smear zones have been widely studied (e.g. Kim and Lee 1997, Zhu and Yin 2000, Cascone and Biondi 2013, Deng et al. 2013, Xue et al. 2014, Chen et al. 2016, Nguyen and Indraratna 2017). However, very few studies exist regarding the long-term effects of PVD installation on the response of the soft soil layer (e.g. Kim 2012, Lo et al. 2013, Hu et al. 2014), this deemed to be in part due to the unavailability of appropriate soil models. Many soil constitutive models, which are commonly used for the analysis and design of geotechnical engineering problems, assume that the behavior of soil is simply isotropic. Application of such simplified models in practice often provide solutions that are overly conservative and costly, and in some cases result in uncertainties regarding long-term performances. In reality, the behavior of natural soils is highly anisotropic. Natural clays also have an inherent structural property that gives them an undisturbed shear strength in excess of their remolded strength. Furthermore, clayey soils are known to be the most susceptible to time effects on their strength and deformation characteristics. An accurate prediction of soft soil response, either improved or unimproved,

requires that these aspects of their behavior are considered by the employed constitutive model.

Because of considerable computational cost of three dimensional (3D) finite element (FE) analysis, the boundary value problems related to PVD ground improvement are commonly modelled in the representative 2D plane-strain condition. However, as the water flow into the PVD is an axisymmetric problem; therefore, for the representative 2D analysis, a number of so-called mathematical matching techniques have been proposed (e.g. Hird et al. 1992, Lin et al. 2000, Indraratna et al. 2005). These matching methods are used for the conversion of the permeability coefficient from axisymmetric state into plane-strain condition.

The aim of this paper is to numerically analyze the long-term effects of PVD installation on the behavior of the improved soft clay deposit, and to verify the accuracy and the consistency of a recently developed creep constitutive model in predicting the consolidation settlements and deformations at a practical level. For this study primarily an advanced creep constitutive model, namely Creep-SCLAY1S (Sivasithamparam et al. 2015), is used for carrying out the numerical analysis. An instrumented embankment on soft clay, namely Haarajoki test embankment (Finish National Road Administration, 1997) is simulated. This test embankment is constructed on deep soft soil deposits improved with PVDs for one half of its length. The results from the newly developed creep model are compared with those obtained by using a time-independent anisotropic model, S-CLAY1S (Karstunen et al. 2005), and the MCC model (Roscoe and Burland, 1968). In addition, a simple comparative study is carried out in order to examine the sensitivity of the results to the adopted matching technique.

2 Creep-SCLAY1S Model

The Creep-SCLAY1 (Sivasithamparam et al. 2015) is an extension of S-CLAY1 (Wheeler et al. 2003) to incorporate rate-dependent response of clays. In this model the elliptical surface of the S-CLAY1 model is adopted as the Normal Consolidation Surface (NCS), i.e. the boundary between small and large irreversible (creep) strains. Furthermore, in this model

creep is formulated using the concept of a constant rate of visco-plastic multiplier (Grimstad et al. 2010). The new creep model incorporates the same rotational hardening law as that of the S-CLAY1 and S-CLAY1S models. Moreover, the Creep-SCLAY1 model has been further extended by incorporating the destructuration hardening law of the S-CLAY1S model to take into account the effect of the initial inter-particle bonding in the soil response. Despite assuming anisotropy of plastic behavior, the S-CLAY1 class of models assume isotropy of elastic behavior which is a reasonable assumption for modelling the behavior of soft and sensitive clays (Rezania et al. 2016a). In addition to the soil parameters required for modelling with SCLAY1S (as detailed in Karstunen et al. 2005), the use of Creep-SCLAY1S requires three viscous parameters namely, the reference time, τ, the modified creep index, μ^*, and the intrinsic value of the modified creep index, μ_i^*. Note that μ^* is related to the one-dimensional secondary compression index, C_α, as

$$\mu^* = C_\alpha/[\ln 10\ (1 + e_0)] \tag{1}$$

The extended Creep-SCLAY1S model has recently been successfully applied for modelling pile installation effects in a soft clay deposits (Rezania et al. 2016b)

3 Numerical modelling of PVD-improved ground

For planning a PVD ground improvement work, penetration depth, installation pattern and spacing of PVDs are the important factors that need to be taken into consideration. For the Haarajoki embankment the length of the PVDs used was 15 m and for simplicity they were installed in a square pattern (Fig. 1a), as opposed to a triangular pattern (Fig. 1b), with a spacing of $S = 1\,m$. The equivalent diameter, D, is the diameter of soil medium that is discharging water into its corresponding PVD and it is calculated based on the spacing S between the PVDs. For the square pattern $D = 1.128S$.

During PVD installation, the insertion and removal of the mandrel modifies the properties of the neighboring soil. This effect mainly concerns the densification and disturbance of soil

99 structure, thus it is known as “smear” effect and the affected zone as “smear zone” (Fig. 1c).
100 The diameter of smear zone, D_s, depends on many factors including size of the mandrel,
101 installation method, the structure of the soil etc. Several studies have been carried out on the
102 determination of D_s (e.g., Xiao 2001), and its value is often considered to be in the range of 3-
103 5 times the diameter of the mandrel, D_m, or 5-8 times the equivalent drain diameter, D_w.

104 Ideally the study of PVD ground improvement is a 3D problem, requiring a 3D FE analysis.
105 However, such a model would be computationally very expensive. Therefore, often a 2D
106 plane-strain FE model is used and a matching technique is employed to convert the general
107 permeability of the medium into an equivalent plane-strain value. In practice, the axisymmetric
108 unit cell representing a drain is simplified into a plane-strain unit cell, assuming an equivalent
109 half width, B, for the cell.

110 A number of simplified matching approaches are available in the literature which are based
111 on manipulation of, either the drain spacing or the soil permeability. For the simplicity of
112 relationships each drain is assumed to work independently, a constant soil permeability is
113 adopted and consolidation is considered to take place in a uniform soil column with linear
114 compressibility characteristics (Yildiz et al. 2009). Comparing the numerical results in
115 literature, it seems that the 2D plane-strain analyses do not give a satisfactory agreement in
116 estimating the maximum value of excess pore pressure after construction. This may be
117 because the geometry and/or the permeability of the domain are changed but the
118 compressibility of the soil itself remains constant. Nonetheless, regardless of this issue, the
119 matching technique proposed by Hird et al. (1992) appears to be the most convenient one as
120 it allows the mesh size to be controlled. Another advantage of this technique is that no
121 particular smear zone is required to be considered in the modelling.

122 A simple permeability matching technique has also been proposed by Lin et al. (2000), where
123 matching is done for the horizontal permeability (see Equation (2))

$$k_{hpl} = \frac{k_h \pi}{6\left[\ln\left(\frac{n}{s}\right) + \frac{k_h}{k_s}\ln(s) - \frac{3}{4}\right]} \quad (2)$$

where k_{hpl} is the equivalent horizontal permeability of surrounding soil in plane-strain condition, k_h is the horizontal permeability of the undisturbed soil, k_s is the horizontal permeability of the smeared zone, $n = R/R_w$ and $s = R_s/R_w$ where R, R_w and R_s are the radius of the unit cell (equivalent radius), the drain, and the smear zone, respectively. In this paper the matching technique proposed by Hird et al. (1992) together with the one proposed by Lin et al. (2000) have been used to carry out numerical analyses.

The drain adopted at the site was reported to have an average width of 98.7 mm with a discharge capacity of 157 m^3/year. The equivalent diameter of the drain, calculated according to the formulation proposed by Hansbo (1979) is 67 mm. Considering for the smear effect the ratios $k_h/k_s = 20$ and $D_s/D_w = 8$, values that proved to give accurate results when used with the advanced constitutive models of the S-CLAY family (Yildiz et al. 2009), the equivalent plane-strain permeability is $k_{hpl} = 0.0126k_h$.

The advanced models, S-CLAY1S and Creep-SCLAY1S, have been implemented into the finite-element code PLAXIS AE (Brinkgreve et al. 2014) through the user-defined soil model facility of the software (Rezania et al. 2014). Details of the simulations carried out, and the analysis of the results, in comparison with field performances, are discussed in the following.

3.1 Haarajoki embankment

Haarajoki embankment has a height of 2.9 m and a length of 100 m. Its crest is 8 m wide and the slopes have a gradient of 1:2. It was founded on a 2 m thick dry crust lying above a 20.2 m thick soft clay deposit. The foundation soil consists of soft soil with a high degree of anisotropy and some inter-particle bonding. Half of the embankment (50-m-long section) was constructed on PVD improved soft soil and the other half was built on the natural soft soil without any ground improvement measure.

A finite element mesh with 6-noded triangular elements is used for the FE analyses, with extra degrees of freedom for excess PWP at corner nodes (during consolidation analysis). Mesh sensitivity studies have been done to ensure that the mesh is dense enough to produce accurate results. The geometry of the FE model is shown in Fig. 2; for the model, the far right boundary is assumed at 40 m distance from the centerline. The bottom boundary of the clay deposit is assumed to be completely fixed in both horizontal and vertical directions; whereas, the left and right vertical boundaries are only restrained horizontally. Drainage is allowed at the ground level, while due to unknown hydraulic conditions at the bottom boundary, this boundary is considered impermeable. Impermeable drainage boundaries are also assigned to the lateral boundaries. Based on ground data, the water table is assumed to be at the ground surface. For the side of the embankment that was built on improved soil, PVDs are incorporated in the model using the drain element in PLAXIS. Groundwater head is assumed to be at ground level for all drains.

The embankment was built in 0.5m thick layers and each layer was placed and compacted within 2 days, except for the foundation layer which was built within 5 days. For the calculation phases, plastic analyses are carried out corresponding to the construction process of the embankment, after which the consolidation analysis is performed.

3.1.1 Parameters estimation

The embankment itself is modelled using the simple linear elastic-perfectly plastic Mohr-Coulomb model with the following reported values for the embankment material: Young modulus $E = 40000$ kPa, Poisson's coefficient $\nu = 0.35$, cohesion $c' = 2$ kPa, friction angle $\phi' = 40°$, unit weight $\gamma = 21$ kN/m^3.

For the numerical simulation, the first layer (0-2 m) is divided into two parts; the first sub-layer (0-1 m) is modelled with the Mohr-Coulomb model using $E = 2300$ kPa, $c' = 1$ kPa and $\phi' = 30°$. The second sub-layer (1-2 m) is modelled by assigning the relative advanced soil

constitutive model used in the analysis without consideration of the effect of soil structure, given that the soil at this layer has low sensitivity due to being fairly disturbed.

Based on the site investigation data and parameter values reported by Karstunen et al. (2015), the soft soil deposit beneath Haarajoki embankment can be sub-divided into seven layers with different parameter values. The values of model constants and state variables used for the different soil layers are summarized in Table 1. In this table the conventional soil constants, such as the elasticity constants κ and ν, and the critical state constants λ, λ_i (i.e., the intrinsic value of λ) and M are the same as those for the MCC model, hence their values are determined in the standard manner. The values of the advanced anisotropic model parameters have been determined following the approaches proposed in Wheeler et al. (2003) (for evaluation of anisotropy parameters α_0, ω and ω_d), and Karstunen et al. (2005) (for evaluation of destructuration parameters χ_0, ζ and ζ_d).

Variation of permeability k with void ratio e during consolidation analysis is represented in simulations through permeability change index parameter c_k which is calculated according to the following equation proposed by Berry and Poskitt (1972)

$$c_k = \frac{e - e_0}{\log\left(\frac{k}{k_0}\right)} \tag{3}$$

The values of the constant c_k can be obtained from the results of the oedometer tests.

For evaluation of the creep parameter, μ_i^*, (Sivasithamparam et al. 2015) the value of creep index, C_α, measured from conventional oedometer test results is used. According to Mesri and Godlewski (1977), the ratio of C_α/λ can be considered to be constant for each clay layer. The intrinsic value of the creep index $C_{\alpha i}$ (the subscript i stands for the intrinsic values) corresponding to the intrinsic compression index λ_i of each layer can be obtained by $C_\alpha\lambda_i/\lambda$. The values of the μ_i^* are essentially derived using the Equation (1). It should be noted that the value of μ_i^* significantly influences the results, therefore its appropriate calibration is essential

for realistic modelling of the long-term behavior. For determination of μ_i^* values based on the abovementioned approach, a number of available laboratory test data were carefully interpreted and the C_α and λ values which provide best simulation results were selected. Finally, the values of modified intrinsic compression and swelling indexes, λ_i^* and κ^*, are obtained as λ_i^*= λ_i*/(1+e)* and κ^*= κ*/(1+e)* with *e* being the void ratio (Leoni et al., 2008). Furthermore, Table 2 summarizes the parameter values used for the calculation of the equivalent plane-strain permeability, according to the employed matching technique. The modified coefficients of permeability of the soil layers, k_{hpl}, are presented in Table 3.

3.1.2 Results and discussion

3.1.2.1 Settlements

Fig. 3a shows settlement predictions versus time at the node directly under the centerline of the embankment (point A in Fig. 2) for the side of the embankment that is not improved with PVDs. It can be seen in the figure that the creep model provides an improved prediction of the field measurements, however it is clearly on the conservative side. MCC grossly underestimates the settlements. It is capable to accurately predict the settlement that occurred in early stages; however, the predicted settlement rate slows down after about day 50, pointing out that the model cannot take into consideration the time-dependent aspect of the soil behavior. Application of S-CLAY1S model leads to a similar settlement prediction trend, but, compared to MCC, it provides a less conservative modelling result as it considers the effects of inherent features of natural soil behavior, particularly destructuration (i.e., strain softening).

Vertical settlement plots calculated for the side of the embankment built on the PVD improved soil are presented in Fig. 3b. It is observed that all three constitutive models capture the effect of PVD installation on accelerating the settlement of the soft ground. Settlement prediction by the Creep-SCLAY1S model matches well with the field observations. It demonstrates that the model is capable of providing an enhanced simulation for complex scenarios where soil strata consists of both undisturbed and disturbed (smear zone) segments combined with drainage elements.

Surface settlement field data is available for the side of the embankment that was built on unimproved soil. The measurements were taken on 10 days, 5 years and 10.7 years after construction. The data has been used to investigate the surface settlement through predictions from different models (see Fig. 4). With regards to the embankment side that was built on the unimproved ground (Fig. 4a), all numerical simulations show limited vertical settlements outside the embankment area; however, Creep-SCLAY1S predicts more surface heaving in this area, particularly in short-term. All three models provide good estimation of the surface settlements shortly after construction (i.e., after 10 days). However, in long-term, MCC model grossly underestimates the surface settlements; while S-CLAY1S provides an improved prediction, although still underestimating the field data. The Creep-SCLAY1S model is able to significantly better capture the field observations, while still underestimating the vertical displacements after 5 and 10 years.

The numerical simulation results for the effect of PVD installation on the surface settlements, up to a distance of 40 m from the centerline of the embankment, can be observed in Fig. 4b. No field data is available for this side of the embankment; hence, the simulation results are presented for the same times when measurements were taken for the other half of the embankment. For all of the soil models, the predicted trends are almost the same as the case without PVDs (see Fig. 4b). The predicted vertical settlement immediately after construction remains very similar to the unimproved side of the embankment; however, for the longer time periods the increased amounts of vertical settlements are apparent, in particular for when the advanced models S-CLAY1S and Creep-SCLAY1S are used.

Estimation of the settlement influence zone is particularly important for planning the construction work in urban areas with dense concentrations of buildings. The span of settlement influence zone predicted by different models is different. For both sides of the embankment the Creep-SCLAY1S model predicts a large influence zone (e.g., about 30 m from the centerline of the embankment on the unimproved side), whereas MCC and S-CLAY1S models clearly predict a smaller influence zone (e.g., up to about 16 m on the

unimproved side). From the figure, the extent of the influence zone seemingly decreases on the side where the vertical drains are installed (see Fig. 4b), for example on this side MCC and SCLAY1S predict an influence zone of less than 10 m and Creep-SCLAY1S predicts an influence zone of less than 30 m.

3.1.2.2 Lateral displacements

For the unimproved side of the embankment, the lateral displacement predictions underneath the crest (4 m from the centerline) of the embankment after 15 days, 1 year and 3 years of consolidation, are presented in Fig. 5a and are compared with the field data. From the results, MCC and S-CLAY1S evidently underestimate the lateral displacements of the soft soil deposit, particularly at higher ground levels. Creep-SCLAY1S is able to accurately predict the maximum value of lateral displacement under the crest; however, for deeper ground levels it overestimates the deformations. This could be partly due to the approximating approach used for the determination of the creep index. All three models are able to predict the depth at which the maximum horizontal displacement occurs (2.5 m), with Creep-SCLAY1S providing more representative predictions.

For the PVD improved side of the embankment, except for the top ground layer, all three models provide reasonably good prediction of the lateral displacements under the embankment crest in short-term (after 15 days consolidation) (Fig. 5b). The relatively large displacement at the field near the ground surface is believed to be caused by error in the field measurements. According to the field data, by comparing the measurements on both sides of the embankment it appears that the installation of PVDs does not result in significant differences on the amount of lateral displacements in short-term.

For the horizontal displacements at the toe of the embankment, generally all three models provide reasonable predictions for the side of the embankment that is built on the unimproved foundation soil (Fig. 6a). Overall, MCC and S-CLAY1S models underestimate the lateral displacements at shallow depths, while Creep-SCLAY1S overestimates the horizontal displacements a year after construction but provides more accurate predictions of lateral

displacements 3 years after construction. Better approximations of the lateral deformations at deeper depths are obtained from the MCC and SCLAY1S models, while Creep-SCLAY1S overestimates the lateral deformations at these depths.

With regards to the part of the embankment that is built on the PVD improved ground, all three models fairly overestimate the amount of lateral displacements under the embankment toe after 3 years of consolidation (Fig. 6b). This could be due to the fact that friction effects between the soft soil and the PVDs are neglected in the numerical simulations. The narrowly spaced PVDs are believed to act as some sort of “reinforcements” that can reduce the long-term lateral displacements.

3.1.2.3 Excess pore pressure

Pneumatic piezometers were installed at different depths underneath the embankment to monitor the excess PWP variations with time. Measurements are available only for the half of the embankment built on the unimproved ground; however, the numerical simulation results of the PWP dissipation are obtained for both sides of the embankment. Fig. 7a shows the *in-situ* measurements of PWP related to piezometers located at a depth of 4 m, 7 m, 10 m, and 15 m under the centerline. The actual pore pressure measurements are rather erratic, not following a regular trend, particularly for the depth of 4 m, therefore the field data should not be assumed as definitive. The excess PWP initially builds up during the embankment construction and then it is gradually dissipated with time. It is seen in Fig. 7a that all three constitutive models overestimate the initial excess PWP build up at 4 m and 7 m depths. However, a relatively accurate prediction of initial excess PWP is obtained at deeper depths i.e. 10 m and 15 m.

Considering the plots of PWP dissipation with time in Fig. 7a, it is observed that the dissipation rate is faster when the isotropic MCC and time-independent SCLAY1S models are used, while the application of the Creep-SCLAY1S results in the slowest rate of excess PWP dissipation. This trend is observed at all depths analyzed here. Note that at 10 m and 15 m depths, the

predictions of Creep-SCLAY1S show an increasing build-up of excess PWP up to day 650 (not shown here) from when the dissipation of excess PWP is commenced.

For the embankment side that was built on the PVD improved ground, all three models initially show a sharp increase in the amount of excess PWP immediately after construction, followed by a faster dissipation rate which is sensible as additional dissipation paths are provided by the PVDs to discharge excess pore pressures (Fig. 7b). The results in Fig. 7 are presented for the first 500 days of consolidation; however, the numerical analysis showed that when the MCC model is used the excess PWP fully dissipated after 3500 days of consolidation, this is the time that according to MCC consolidation settlement stops progressing. When S-CLAY1S and Creep-SCLAY1S models are used the PWP dissipation prolongs into the following years which is why with these models the consolidation settlement is continually progressing.

3.1.2.4 Stress field and state parameters

The installation of vertical drains also alters the stress field underneath the embankment. The presence of drains leads to an increase in the stress values in the region near the drains, while far from the drains the stress field approximately returns to that of the field underneath the embankment without PVDs. This behavior has been observed for both vertical and horizontal stresses; Fig. 8a shows the stress distribution along the embankment foundation 15 days after construction and at a depth of 2.7 m, using the Creep-SCLAY1S model. The same behavior, but with lower peaks at the drain locations, is observed for when several years of consolidation have passed. Note that, due to the close spacing of PVDs, directly underneath the embankment the effective mean stress values are continually increasing and decreasing.

Along with the stress field, column installation also influences the state parameters of the soil such as void ratio. Void ratio decreases near the drains (see Fig. 8b) indicating a densification of the soil due to fast drainage in this area. In between the drains, the value of the void ratio increases, but it does not reach the values corresponding to when the foundation soft soil is unimproved.

In a similar manner, the presence of PVDs influences the structure of the soil. Considering destructuration parameter χ (Fig. 8c), the presence of drains causes a decrease of this state parameter at the proximity of the drains, which is likely to be due to the disturbance caused by the presence of the drain. The recovery in between the drains does not reach the values of the simulation without PVDs.

3.2 Matching techniques

As discussed earlier, different matching techniques can be adopted to calculate the equivalent permeability for the soil deposit when PVDs are installed. In this study the applications of two different matching techniques are compared, one is a popular method proposed by Hird et al. (1992) and the second is a less known method proposed by Lin et al. (2000). Considering the parameters presented in Table 3, the equivalent permeability with the matching technique proposed by Lin et al. (2000) is obtained as $k_{pl} = 0.012k_h$, which is a value very close to the one obtained with the formulation of Hird et al. (1992).

Comparing the long-term settlement plots of the two sides of the case study embankment studied in this paper (Fig. 9a) the numerical results obtained using the two matching techniques are very similar. Also in terms of lateral deformations, the difference between the results corresponding to the application of the two matching techniques is not noticeable (Fig. 9b). It is difficult to point out which is the more appropriate matching technique as the results are almost identical.

When adopting the combined matching technique of Hird et al. (1992), one has to preselect the value of the width of the equivalent plane-strain unit cell in order to obtain the corresponding permeability, as the model takes into account both geometry and permeability factors. By changing the value of B, in this instance for example adopting $B = 1$, the permeability value changes accordingly ($k_{pl} = 0.0504k_h$). It is observed that greater spacing between the drains leads to a remarkable increase in settlement predictions (Fig. 10a). Distribution of the effective stress parameter is slightly influenced by increase in drain spacing,

resulting in lower decrease/increase of stresses within the PVD improved soil (Fig. 10b). Variations of the state parameters e and χ are also decreased with increase in drain spacing (Figs. 10c and d). In fact, higher values of equivalent plain-strain permeabilities obtained from using higher drain spacing leads to a higher rate of consolidation and consequently higher degradation of the inter-particle bonds (destructuration) within the PVD improved area. The recovery in between the drains does not reach the values of the simulation with $B = 0.5$. An advantage of assuming a greater value of B is the possibility to better control the FE mesh, adopting a less refined mesh, therefore increasing the efficiency of the simulation.

As in the formulation of the equivalent plain-strain permeability proposed by Lin et al. (2000) the geometry of the model is not considered, adopting different values for the equivalent plane-strain cell does not alter the predictions. This implies that no further simplification of the numerical model is feasible when the matching technique of Lin et al. (2000) is used. Therefore, adopting an equivalent plain-strain width ($2B$) equal to the drain spacing (S) is necessary for modelling PVD improved soil foundations.

4 Conclusions

In this paper, the influence of prefabricated vertical drains (PVDs) installation on the consolidation response of the soft soils is analyzed. A case study test embankment namely Haarajoki embankment is taken into consideration. Three different soil constitutive models are applied for the numerical simulations (MCC, S-CLAY1S and the newly developed Creep-SCLAY1S) in order to highlight the importance of considering time-effects (i.e., creep) in natural soil behavior at practical level.

Based on the results, the Creep-SCLAY1S model appeared to be capable of providing reasonably accurate predictions of the delayed soft soil response in general, and the PVD installation effects in particular. The inability of the MCC and S-CLAY1S models to reproduce the delayed response of the clay makes these models noticeably unviable for modelling case studies where the soil response is considerably prone to creep. Furthermore, given the

influence of the modified creep parameter values for accurate modelling of progressive deformations with the Creep-SCLAY1S model, the good agreement between the creep model predictions and observed settlements indicates that, where direct test data is not available, the adopted methodology (i.e., $C_{\alpha i} = C_{\alpha}\lambda_i/\lambda$) for estimation of intrinsic creep index values is reasonably reliable for practical applications.

Concerning the numerical results for lateral deformations (see Fig. 5) there are clear discrepancies between model predictions and field data at the ground level which could be due to errors during lateral deformation measurements at the surface of the ground.

From the results presented, it could be observed that embankment loading combined with prefabricated vertical drains is a very effective ground improvement technique for soft soil deposits. In fact, the installation of PVDs significantly accelerates the settlement of soft clays and the process of excess pore pressure dissipation. In this way, the construction project can proceed faster without further damaging settlements in subsequent years. Additionally, the presence of vertical drains alters the stress field and the soil state parameters, leading to a higher stress level in the PVD improved area as well as further densification of the soil.

The actual field condition around vertical drains is 3D; therefore, a comprehensive analysis of an embankment built over a soil deposit with a large number of PVDs should be conducted with a fully three dimensional numerical model. However, an appropriate matching technique to convert the vertical drain system into equivalent plane-strain condition allows using a representative 2D plane-strain model, which is computationally less expensive. Two different matching techniques, proposed by Hird et al. (1992) and Lin et al. (2000), have been adopted for the numerical simulations in this study, and it was observed that their application leads to fairly similar results. Nevertheless, the matching technique proposed by Hird et al. (1992) appears to be more versatile as it takes into account both geometry and permeability aspects, and as such its application allows to better control the efficiency of the numerical simulation.

References

Abuel-Naga, H.M., Bergado, D.T., Gniel, J., 2015. Design chart for prefabricated vertical drains improved ground. Geotext. Geomemb. 43, 537–546.

Berry, P. L., and Poskitt, T. J., 1972. The consolidation of peat. Géotechnique 22 (1), 27-52.

Brinkgreve R.B.J., Engin E., Swolfs W.M., 2014. Plaxis 2014 reference manual, Plaxis, Delft, Netherlands.

Cascone, E., Biondi, G., 2013. A case study on soil settlements induced by preloading and vertical drains. Geotext. Geomemb. 38, 51–67.

Chen, J.F., Tolooiyan, A., Xue, J.F., Shi, Z.M., 2016. Performance of a geogrid reinforced soil wall on PVD drained multilayer soft soils. Geotext. Geomemb. 44 (3), 219–229.

Deng, Y.B., Xie, K.H., Lu, M.M., Tao, H.B., Liu, G.B., 2013. Consolidation by prefabricated vertical drains considering the time dependent well resistance. Geotext. Geomemb. 36, 20–26.

Finnish National Road Administration, 1997. Competition to calculate settlements at the Haarajoki test embankment. Competition programme, competition materials, Finnra, Helsinki, Finland.

Grimstad, G., Abate, S., Nordal, S., Karstunen, M., 2010. Modeling creep and rate effects in structured anisotropic soft clays. Acta Geotechnica 5, 69–81.

Hansbo, S., 1979. Consolidation of clay by band-shaped vertical drains. Ground Eng. 12 (5), 16–25.

Hird C.C., Pyrah I.C., Russell D., 1992. Finite element modeling of vertical drains beneath embankments on soft ground. Géotechnique 42 (3). 499–511.

Hu, Y.Y., Zhou, W.H., Cai, Y.Q., 2014. Large-strain elastic viscoplastic consolidation analysis of very soft clay layers with vertical drains under preloading. Can. Geotech. J. 51, 144–157.

Indraratna, B., Sathananthan, I., Rujikiatkamjorn, C., Balasubramaniam A. S., 2005. Analytical and numerical modelling of soft soil stabilized by PVD incorporating vacuum preloading. Int. J. Geomech. 5 (2), 114–124.

Karstunen, M., Krenn, H., Wheeler, S. J., Koskinen, M., Zentar, R., 2005. The effect of anisotropy and destructuration on the behaviour of Murro test embankment. Int. J. Geomech. 5 (2), 87–97.

Karstunen, M., Rezania, M., Sivasithamparam, N., Yin, Z-Y., 2015. Comparison of anisotropic rate-dependent models for modeling consolidation of soft clays. Int. J. Geomech. 15 (5), 1–11.

Kim, Y.T., 2012. Strain rate-dependent consolidation behaviors of embankment with or without vertical drains. Marine Georesour. Geotech. 30 (4), 274–290.

Kim, Y.T., Lee, S.R., 1997. An equivalent model and back-analysis technique for modelling in situ consolidation behavior of drainage-installed soft deposits. Comp. Geotech. 20 (2), 125–142.

Lam, L.G., Bergado, D.T., Hino, T., 2015. PVD improvement of soft Bangkok Clay with and without vacuum preloading using analytical and numerical analyses. Geotext. Geomemb. 43, 547–557.

Leoni, M., Karstunen, M., and Vermeer, P.A., 2008. Anisotropic creep model for soft soils. Géotechnique 58 (3), 215–226.

Lin D.G., Kim H.K., Balasubramaniam A.S., 2000. Numerical modelling of prefabricated vertical drain. Geotech. Eng. J. of SEAGS 31 (2), 109–125.

Lo, S.R., Karim, M.R., Gnanendran, C.T., 2013. Consolidation and creep settlement of embankment on soft clay: prediction versus observation. In: Geotechnical Predictions and Practice in Dealing with Geohazards. Springer Netherlands, 77–94.

Mesri, G., Godlewski, P.M., 1977. Time and stress-compressibility interrelationship. J. Geotech. Eng-ASCE 103 (5), 417–430.

Nguyen, T.T., Indraratna, B., 2017. Experimental and numerical investigations into hydraulic behaviour of coir fibre drain. Can. Geotech. J. 54 (1), 75-87

458 Rezania, M., Sivasithamparam, N., and Mousavi-Nezhad, M., 2014. On the stress update
459 algorithm of an advanced critical state elasto-plastic model and the effect of yield
460 function equation. Finite Elem. Anal. Des. 90, 74-83.
461 Rezania, M., Taiebat, M. and Poletti, E., 2016a. A viscoplastic SANICLAY model for natural
462 soft soils. Comp. Geotech. 73, 128-141.
463 Rezania, M., Mousavi-Nezhad, M., Zanganeh, H., Castro, J., Sivasithamparam, N., 2016b.
464 Modelling pile setup in natural clay deposit considering soil anisotropy, structure, and
465 creep effects: Case study. Int. J. Geomech. 04016075, 1–13.
466 Roscoe, K.H., Burland, J.B., 1968. On the generalized stress-strain behaviour of 'wet' clay.
467 Engineering plasticity, Cambridge University Press, Cambridge, U.K. 553–609.
468 Rowe, R.K., Taechakumthorn, C., 2008. Combined effect of PVDs and reinforcement on
469 embankments over rate-sensitive soils. Geotext. Geomemb. 26, 239–249.
470 Wheeler, S.J., Näätänen, A., Karstunen, M., Lojander, M., 2003. An anisotropic elastoplastic
471 model for soft clays. Can. Geotech. J. 40, 403–418.
472 Sivasithamparam, N., Karstunen M., Bonnier, P., 2015. Modelling creep behaviour of
473 anisotropic soft soils. Comp. Geotech. 69, 46–57.
474 Wang, J., Cai, Y. Ma, J., Chu, J., Fu, H., Wang, P., Jin, Y., 2016. Improved vacuum preloading
475 method for consolidation of dredged clay-slurry fill. J. Geotech. Geoenviron. Eng.
476 06016012, 1–5.
477 Xiao, D.P., 2001. Consolidation of soft clay using vertical drains. Ph.D. Thesis, Nanyang
478 Technological University, Singapore.
479 Xue, J-F., Chen, J-F., Liu, J-X. , Shi, Z-M., 2014. Instability of a geogrid reinforced soil wall on
480 thick soft Shanghai clay with prefabricated vertical drains: A case study. Geotext.
481 Geomemb. 42, 302–311.
482 Yildiz, A., Karstunen, M., and Krenn, H., 2009. Effect of anisotropy and destructuration on
483 behaviour of Haarojoki test embankment. Int. J. Geomech. 153–165.

484 Zhu, G. and Yin, J.H., 2000. Finite element consolidation analysis of soils with vertical drain.
485 Int. J. Numer. Anal. Met. 24 (4), 337–366.
486

List of notations

B	Half width of plane-strain unit cell	α_0	Initial value of anisotropy
c'	Cohesion	α	Scalar value of anisotropy
c_k	Permeability change index	β	Creep exponent
c_α	Creep index	χ	Bonding parameter
$c_{\alpha i}$	Intrinsic creep index	χ_0	Initial value of bonding parameter
D	Equivalent diameter of unit cell	γ	Unit weight
D_m	Equivalent diameter of mandrel	κ	Slope of swelling/recompression line from $e - lnp_0$diagram
D_s	Equivalent diameter of smear zone	κ^*	Modified slope of swelling/recompression line from $e - lnp_0$diagram
D_w	Equivalent diameter of drain	λ	Slope of post yield compression line from $e - lnp_0$diagram
E	Young's modulus	λ_i	Slope of intrinsic post yield compression line from $e - lnp_0$diagram
e_0	Initial void ratio	λ^*	Modified slope of post yield compression line from $e - lnp_0$diagram
e	Void ratio	λ_i^*	Modified slope of intrinsic post yield compression line from $e - lnp_0$diagram
K_0	coefficient of lateral earth pressure at rest	μ^*	Modified creep index
k	Permeability	μ_i^*	Intrinsic modified creep index
k_h	Horizontal permeability of undisturbed soil	ω	Rate of rotation
k_{hpl}	Equivalent plane-strain horizontal permeability	ω_d	Rate of rotation due to deviator stress
k_s	Horizontal permeability of smear zone	ζ	Parameter controlling absolute rate of destructuration
k_v	Vertical permeability of undisturbed soil	ζ_d	Parameter controlling relative effectiveness of destructuration rate
M	Stress ratio at critical state	ν	Poisson's coefficient
R	Equivalent radius of unit cell	ϕ'	Friction angle
R_s	Equivalent radius of smear zone	τ	Reference time
R_w	Equivalent radius of drain	NCS	Normal consolidation surface
S	Drain spacing	POP	Pre-overburden pressure

Table 1 – Model constants adopted for Haarajoki clay layers

Type	Parameter	Layer 1a (0-1m)	Layer 1b (1-2m)	Layer 2 (2-6m)	Layer 3 (6-7m)	Layer 4 (7-12m)	Layer 5 (12-15m)	Layer 6 (15-18m)	Layer 7 (18-22.2m)
Initial stress state	e_0	1.25	1.25	2.90	2.60	2.35	2.20	2.00	1.25
	γ (kN/m^3)	17.5	17.5	14.3	14.3	15.1	15.1	15.7	17.5
	POP (kN/m^2)	110	32	32	32	32	32	32	32
Elasticity	ν	0.2	0.2	0.2	0.2	0.2	0.2	0.2	0.2
	κ	--------	0.010	0.010	0.030	0.036	0.030	0.034	0.004
Critical State	M	--------	1.60	1.15	1.43	1.15	1.20	1.55	1.55
	λ	--------	0.20	1.33	0.96	0.96	1.06	0.45	0.10
	λ_i	--------	0.20	0.38	0.27	0.26	0.30	0.13	0.03
Anisotropic	α_0	--------	0.63	0.44	0.55	0.44	0.46	0.61	0.61
	ω	--------	37	33	49	44	35	36	37
	ω_d	--------	1.02	0.70	0.97	0.70	0.76	1.01	1.01
Destructuration	χ_0	--------	4	22	30	45	45	45	45
	ζ	--------	8	8	8	8	8	8	8
	ζ_d	--------	0.2	0.2	0.2	0.2	0.2	0.2	0.2
Viscosity	μ^*	--------	1.16E-3	4.44E-3	3.47E-3	3.73E-3	4.32E-3	1.95E-3	5.79E-3
Permeability	$k_h\ (m/d)$	3.46E-4	3.46E-4	1.04E-4	8.64E-5	8.64E-5	8.64E-5	8.64E-5	3.46E-4
	$k_v\ (m/d)$	1.73E-4	1.73E-4	5.18E-5	4.32E-5	4.32E-5	4.32E-5	4.32E-5	1.73E-4
	c_k	0.45	0.45	1.12	1.29	0.74	0.61	0.40	0.40

Table 2 – Parameters adopted for matching technique

S [m]	B [m]	R [m]	R_s [m]	R_w [m]	R_s/R_w	k_h/k_s
1	0.5	0.564	0.268	0.034	8	20

Table 3 – Modified coefficients of permeability according to the matching techniques

Layer	Layer 1a (0-1m)	Layer 1b (1-2m)	Layer 2 (2-6m)	Layer 3 (6-7m)	Layer 4 (7-12m)	Layer 5 (12-15m)	Layer 6 (15-18m)	Layer 7 (18-22.2m)
k_{hpl} (Hird et al. 1992)	4.36E-6	1.31E-6	1.09E-6	1.09E-6	1.09E-6	1.09E-6	1.09E-6	4.36E-6
k_{hpl} (Lin et al., 2000)	4.15E-6	1.25E-6	1.04E-6	1.04E-6	1.04E-6	1.04E-6	1.04E-6	4.15E-6

500

501

502

503

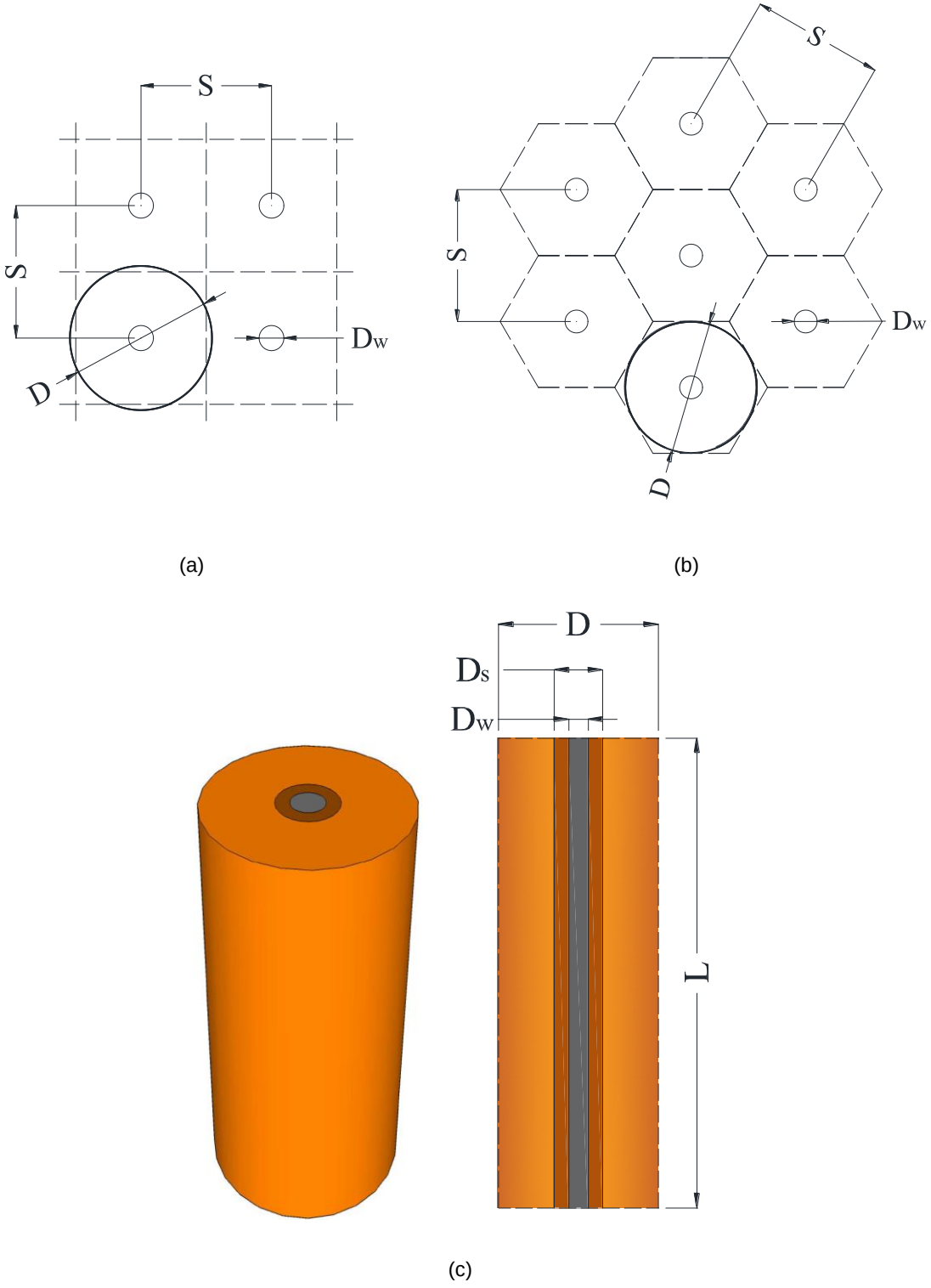

504 Fig. 1. PVD pattern: (a) square pattern; (b) triangular pattern; (c) drain with smear zone

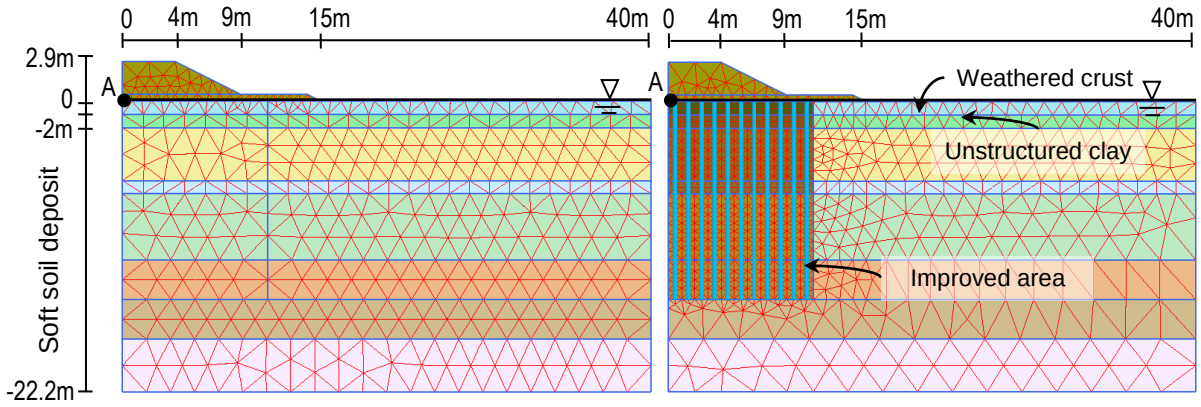

Fig. 2. Geometry of the finite element models adopted for the simulation of Haarajoki test embankment and the position of PVDs; Left: unimproved side; Right: improved side of the foundation soil

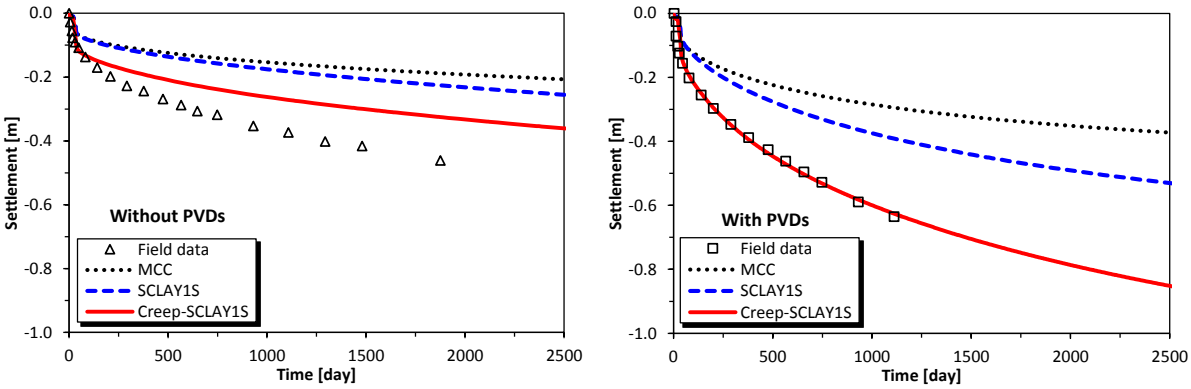

(a) (b)

Fig. 3. Time- settlements plots for Haarajoki embankment at centreline: (a) without PVDs; (b) with PVDs

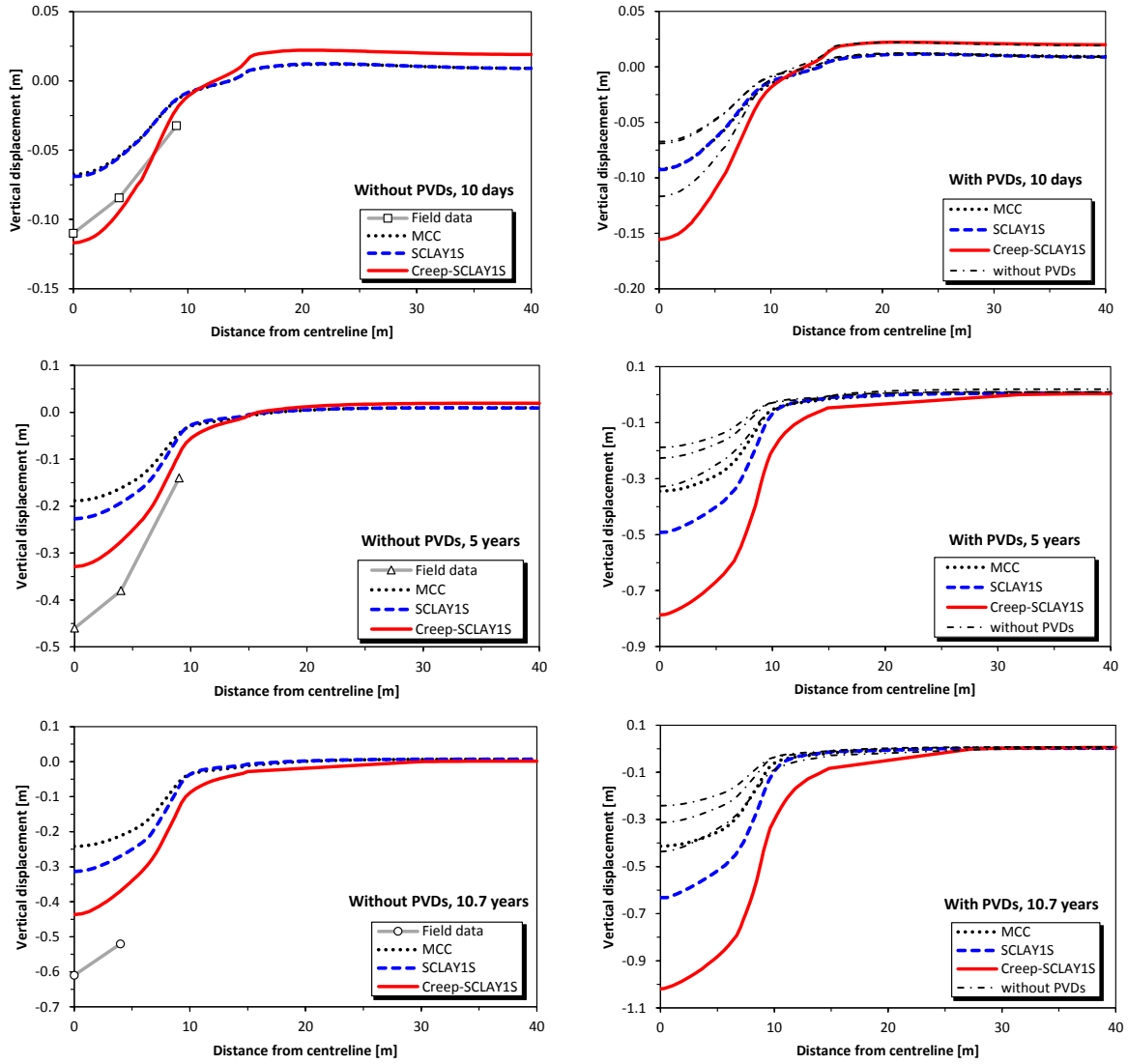

Fig. 4. Surface settlement throughs for Haarajoki embankment: (a) without PVDs; (b) with PVDs

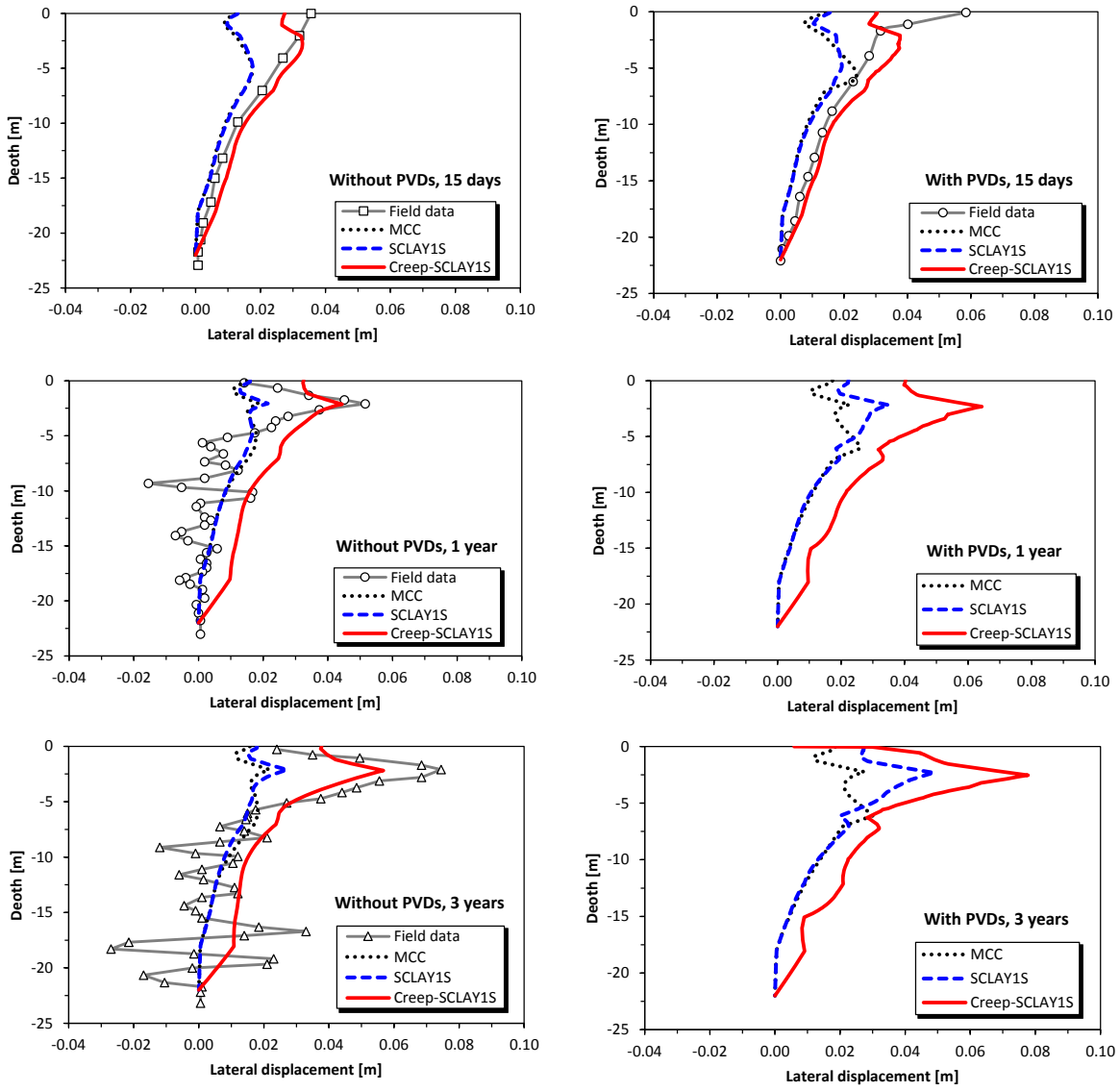

Fig. 5. Lateral displacement predictions for Haarajoki embankment under the crest: (a) without PVDs (b) with PVDs

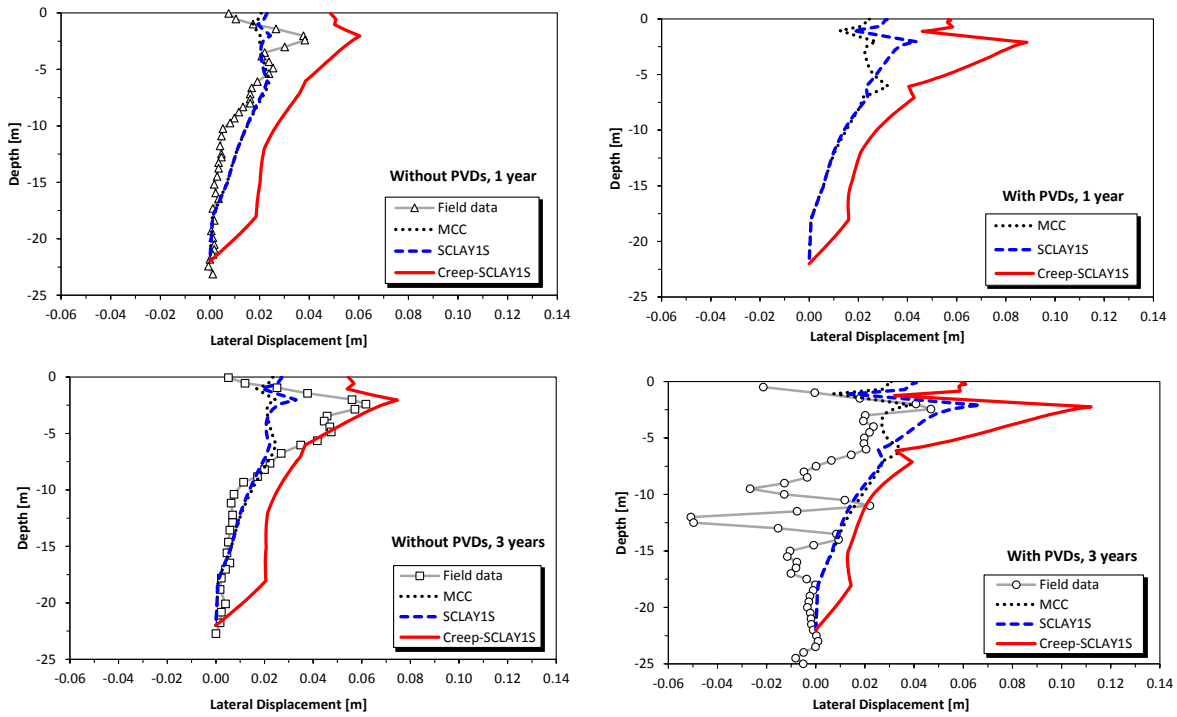

Fig. 6. Lateral displacements predictions for Haarajoki embankment under the toe: (a) without PVDs; (b) with PVDs

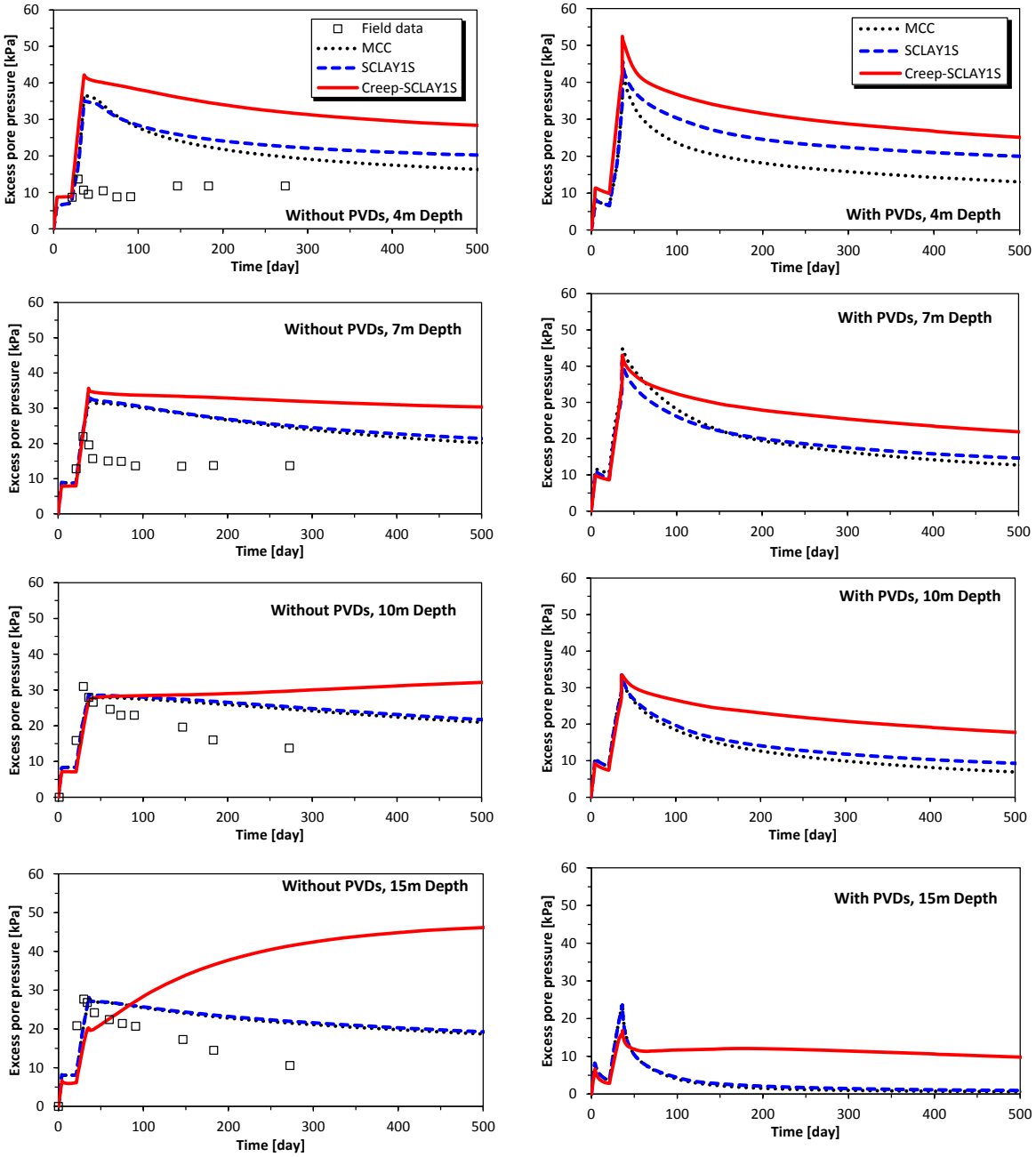

Fig. 7. Excess pore water pressure dissipation with time at different depths: (a) without PVDs; (b) with PVDs

545

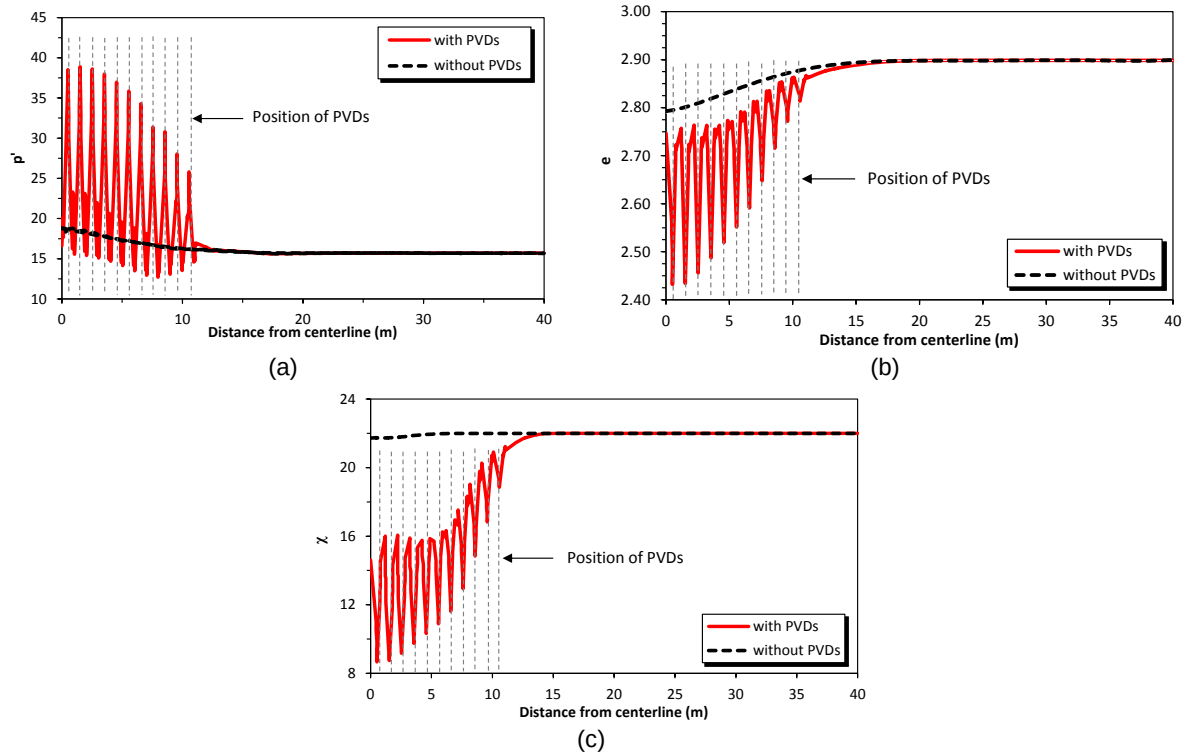

546 Fig. 8. Effect of installation of vertical drains: (a) effective mean stress distribution 15 days after construction; (b)

547 void ratio distribution 1 year after construction; (c) bonding parameter distribution 1 year after construction

548

549

550

551

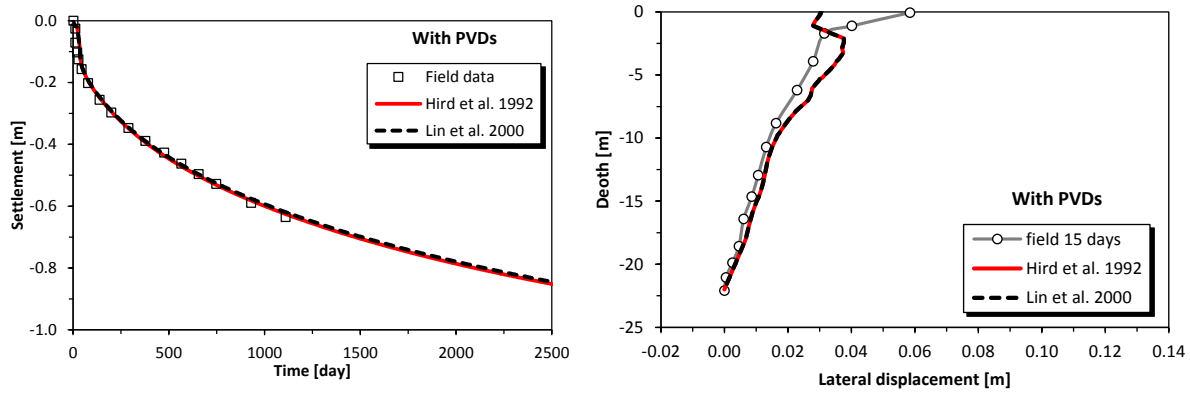

(a) (b)

552 Fig. 9. Comparison of matching techniques: (a) settlements; (b) lateral displacements

553

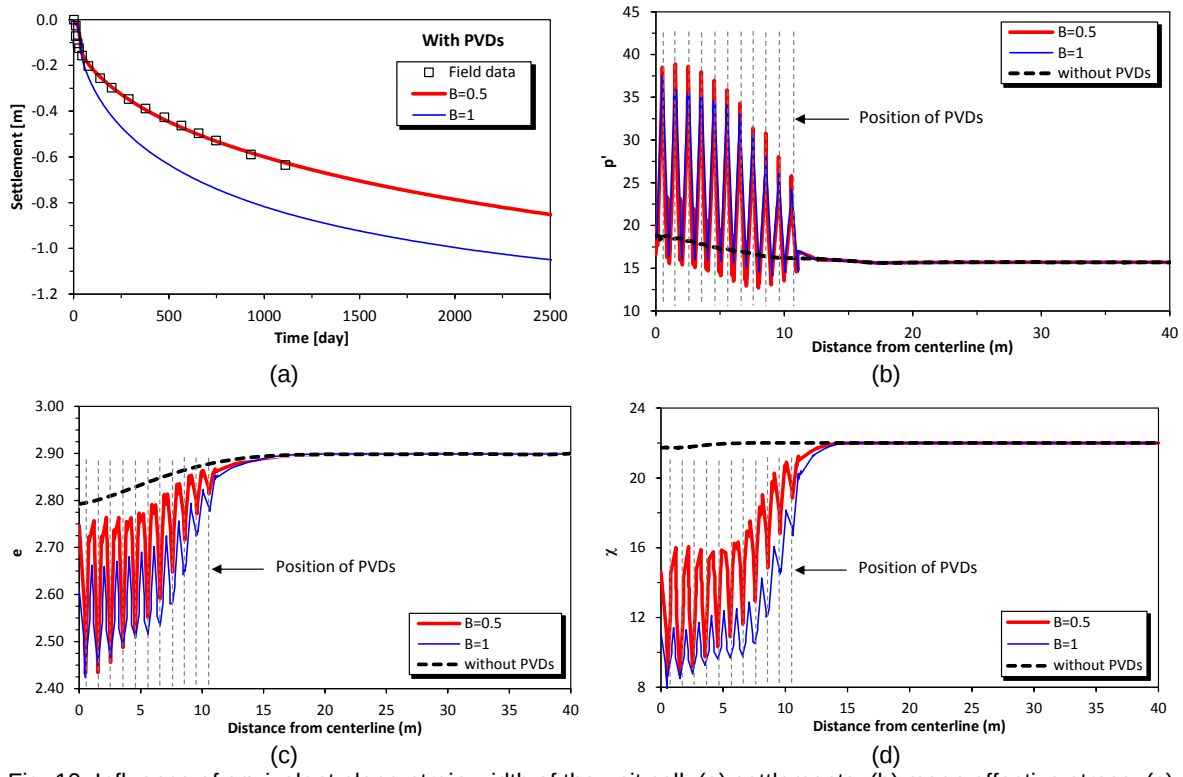

Fig. 10. Influence of equivalent plane-strain width of the unit cell: (a) settlements; (b) mean effective stress; (c) void ratio; (d) bonding parameter